

# System Modelling and Bulk Modulus Estimation of an Electrohydrostatic Actuator

Y. Song, S. A. Gadsden, S. A. El Delbari, and S. R. Habibi

Centre for Mechatronics and Hybrid Technology Research

Department of Mechanical Engineering, McMaster University, Canada

[songy@mcmaster.ca](mailto:songy@mcmaster.ca), [gadsden@mcmaster.ca](mailto:gadsden@mcmaster.ca), [delbarsa@mcmaster.ca](mailto:delbarsa@mcmaster.ca),

and [habibi@mcmaster.ca](mailto:habibi@mcmaster.ca)

## ABSTRACT

An electrohydrostatic actuator (EHA) is an emerging type of actuator typically used in the aerospace industry. EHAs are self-contained units comprised of their own pump, hydraulic circuit, and actuating cylinder. The main components of an EHA include a variable speed motor, an external gear pump, an accumulator, inner circuitry check valves, and a cylinder (or actuator). This article presents the system modelling of an EHA built for experimentation. The system has been built to study a variety of different faults (friction, leakage, and bulk modulus); and models were obtained mathematically, and through system identification. Furthermore, using these system models, this article studies the results of estimating the bulk modulus by implementing the extended Kalman filter (EKF) algorithm.

## 1 Brief Introduction

Hydraulic actuation techniques have been developed and well-studied for decades [1,2,3]. Despite its high power-to-weight ratio, the demand of conventional hydraulics has fallen due to its limitations of control precision, energy efficiency, leakage, and noise [4,5,6]. A new pump controlled, hydraulic actuating technique referred to as an electrohydrostatic actuator (EHA) has been developed since 1990 [4,6]. Compared to conventional valve controlled hydraulic systems; advantages of the EHA system include more precise controllability and higher energy efficiency [7]. A model library that is able to describe the EHA dynamics is required for fault detection and control purposes. In this paper, models are obtained by implementing two modeling techniques: mathematical modelling and system identification. Mathematical models were generated based on a system model in which the parameters have physical meanings. An advantage of this modelling method is that it helps users understand the dynamic effect of each physical parameter in the system. By performing system identification modelling, an empirical black box model is extracted statistically [8]. It does not require full knowledge of the target system; however, the resulting system transfer function has no physical meaning [9].

In this paper, an EHA built for experimentation is studied. Models are generated based on mathematical equations and system identification. Section 2 describes the EHA in more detail, followed by a section on the classification of working and fault conditions. Section 4 provides EHA modelling based on system identification. Mathematical models of the EHA are created in Section 5. These models are validated in Section 6. The EHA bulk modulus is estimated using the extended Kalman filter (EKF), and the results are shown in Section 7. The main findings of the paper are then summarized in the conclusion.

## 2 Electrohydrostatic Actuator

An EHA is an emerging type of actuator typically used in the aerospace industry. EHAs are self-contained units comprised of their own pump, hydraulic circuit, and actuating cylinder [10]. The main components of an EHA include a variable speed motor, an external gear pump, an accumulator, inner circuitry check valves, a cylinder (or actuator), and a bi-directional pressure relief mechanism. The schematic of the EHA circuitry is shown in the Figure 1, as presented in [11]. The EHA can be divided into two subsystems. The first is the inner circuit that includes the accumulator and its surrounding check valves. The second is the high pressure outer circuit which performs the actuation. The inner circuit prevents cavitation which occurs when the inlet pressure reaches near vacuum pressures and provides make-up fluid for any dynamic leakage [10].

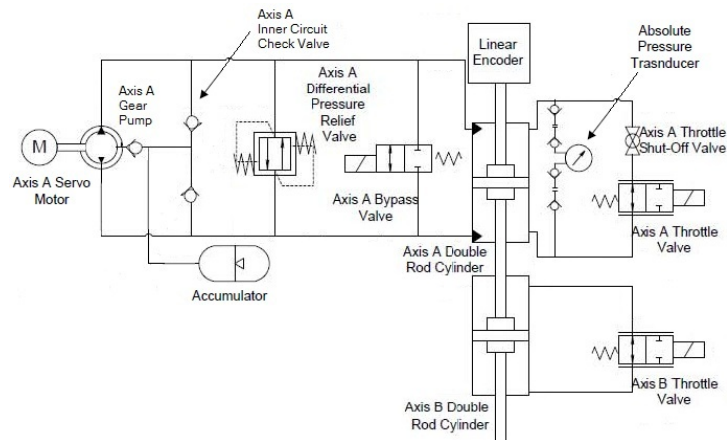


**Figure 1. EHA circuit diagram**

In Axis A, a bi-directional gear pump driven by a servo motor forces fluid to flow from one chamber of the cylinder to the other. The pressure difference generated between chambers starts the actuator movement which is captured by the linear encoder. Besides the position, the pressure difference between chambers is also measured by the absolute pressure transducer. An inner circuit consists of three check valves, and an accumulator collects the leakage from the gear pump case strain and prevents cavitation of the system by maintaining the system pressure above 40 *Psi*. A differential pressure relief valve was installed to prevent the system pressure from exceeding 500 *Psi*, and a bypass valve was set up as a pump fail safe [12].

The EHA experimental setup is shown in the Figure 2. The cylinder on the right (foreground) is referred to as Axis A and the cylinder connected to it on the left (foreground) is referred to as Axis B. An optical linear encoder attached to Axis A is used to obtain position measurements (which are differentiated to obtain velocity measurements). The gear pump and electric motor are located in the rear (middle) of the table. The electric motor drives the gear pump, which moves the hydraulic fluid throughout the circuit. A voltage input controls the direction and speed of the pump which affects the velocity of the cylinders (or actuators). This setup is a closed hydrostatic circuit [13]. More details on the design and setup of the EHA may be found in [14,11,12,13]. The computer and electrical cabinet are located off-camera to the right of the setup. The software used to communicate with the EHA setup is MATLAB's Real-Time Windows Target environment.

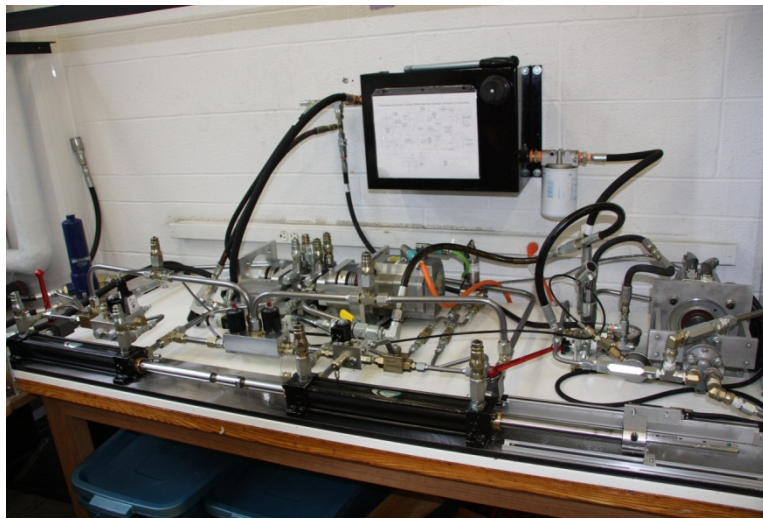


**Figure 2. EHA experimental setup**

### **3 Classification of Working and Fault Conditions**

In this section, the working and fault conditions of the EHA are classified. Two faults (friction and internal leakage) are simulated by connecting chambers of cylinders through throttle valves. The throttle valve selected is the SP08-25 2-way proportional valve from Hydraforce. The SP08-25 valve has its open area controlled by the input voltage. With a maximum 10 V input, the valve is fully closed. In contrast, the valve has the largest flow rate ( $2.57 \times 10^{-3} \text{ m}^3/\text{s}$ ) with a minimum 0 V input. When the Axis A motor drives the actuator to move, the fluid in the Axis B cylinder flows from one chamber to the other through the Axis B throttle valve freely if the valve is set as fully open. In this scenario, a negligible load is generated in Axis B and the system is considered as working normally. As the input converges to 10 V, the throttle valve is partially closed and starts to block the flow. The additional load increases in Axis B and resists the driving axis until the throttle valve is fully closed which leads the system to stall. This additional load is considered as the simulated friction in the EHA system.

A throttle valve connects chambers of the Axis A cylinder in order to simulate internal cross port leakage. When the throttle valve is fully closed, a negligible amount of flow is able to move from one chamber to the other, and the system is considered as working normally. However, when fluid flows cross those chambers while the throttle valve is partially open, one has the internal cross port leakage case. The amount of internal leakage and friction force can be modified and controlled by the throttle valves in Axis A and Axis B, respectively.

Since the EHA system has different dynamic performances with different levels of faults involved, the EHA system working conditions are classified into nine categories: normal, minor leakage, major leakage, minor friction, major friction, and four combined faults conditions; such as minor leakage plus minor friction, major leakage plus minor friction and so forth. The increase of leakage flow causes less flow rate on the main circuit and results in a decrease of actuator velocity. Therefore, the actuator velocity is used to define the level of leakage fault. The system is run under different levels of leakage by keeping the Axis B throttle valve fully open, as shown in the Figure 3. The x-axis refers to the throttle valve designed flow rate which corresponds to the throttle valve control input, while the y-axis refers to the actuator velocity. The minor and major leakage conditions are defined as when the system has nearly 75% and 50% of its normal performance, respectively. Based on Figure 3, the minor leakage fault condition is chosen with a throttle valve input of 2.1 V. The major leakage fault condition is chosen with a throttle valve input of 1.9 V.

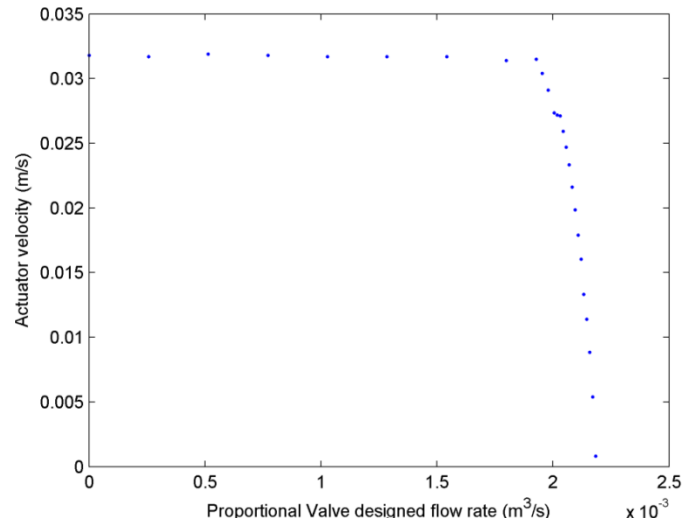


**Figure 3. Methodology for defining the leakage levels**

The decrease of Axis B throttle valve open area causes higher viscosity friction in the flow line and generates a higher pressure difference between the chambers in both cylinder A and B. In order to involve the overall friction force, the pressure difference in cylinder A is used to define the friction fault level.

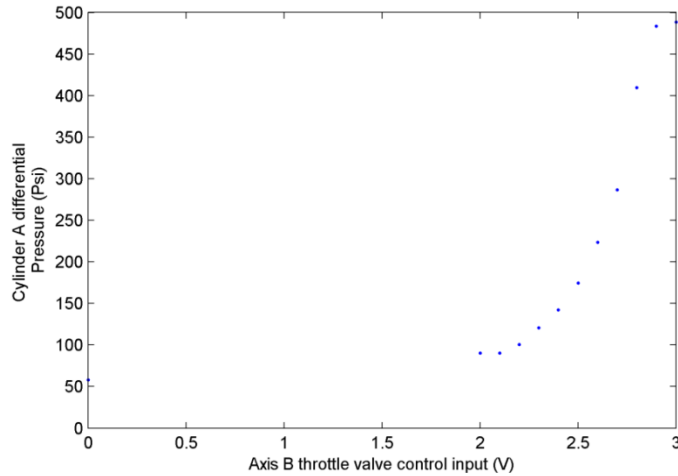


**Figure 4. Methodology for defining the friction levels**

As demonstrated in the Figure 4, the Axis A cylinder differential pressure increases from 58 *Psi* (399.91 *kPa*) as the Axis B throttle valve control input increases until it is saturated at the pressure relief valve activated pressure of 500 *Psi* (3,447.5 *kPa*). Similar to the definition of the leakage fault level, the minor and major friction fault condition are defined as 200% and 300% of the differential pressure at normal case. All of the working conditions that are studied in this paper and their corresponding throttle valve inputs are summarized in the following table.

Table 1. Summary of Working Conditions and Inputs

Working Condition	Axis A Input (V)	Axis B Input (V)
Normal Operation	10	0
Minor Leakage	2	0
Major Leakage	1.75	0
Minor Friction	10	2.3
Major Friction	10	2.5
Minor Leakage and Minor Friction	2	2.3
Major Leakage and Minor Friction	1.75	2.3
Minor Leakage and Major Friction	2	2.5
Major Leakage and Major Friction	1.75	2.5

#### 4 EHA Modelling by System Identification

A complete system identification process involves three main stages. In the first tests stage, the target system is tested to obtain prior knowledge including the system delay, steady state gain, break frequency, system piece-wise linearity, and system order. In the second stage, data collection, the most crucial element is the test signal designed based on the prior

knowledge. A well-designed test signal would help to collect data in the system linear region with proper frequency range. After signal processing, the noisy collected data is filtered and ready to be used in the third stage, model fitting and validation. In the model fitting stage, four model structures are fitted and validated to obtain the most accurate model. The root mean square error (RMSE) is calculated to validate the accuracy of the models. A similar system identification process has been completed with the EHA system by Kevin McCullough in [12]. A third order model was obtained for the system working normally. In this paper, the system identification process is repeated and extended to obtain a model library for the EHA system working under the various conditions defined in Table 1. The results in the latest first tests generally agree with the findings in [12], except for the system piece-wise linearity and order of the model.

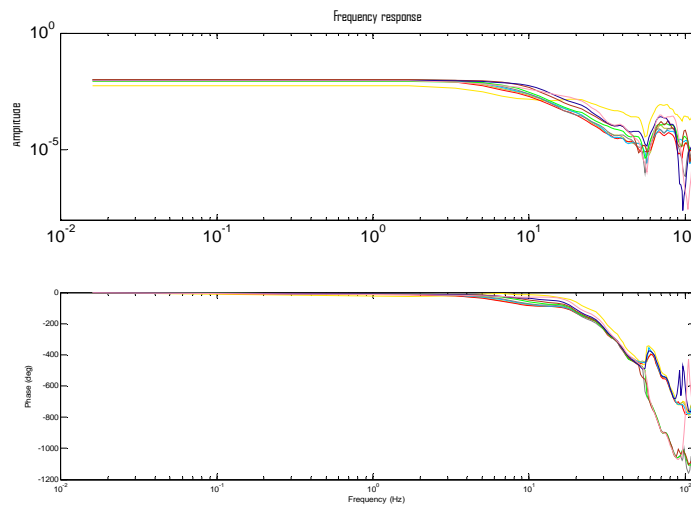


**Figure 5. Frequency response curves (amplitude and phase)**

The above figure demonstrates the updated test result of the system piece-wise linearity about various input means for systems working under the normal scenario. The coloured curves are smoothed empirical transfer function estimate (ETFTE) curves of the system working with motor voltage input means from 0 V to 8 V. Both of the curves result from the actuator velocity over the motor voltage. These curves generally share the same shape which indicates that the system performs linearly with changing input mean. The test is repeated again for systems operated with various input amplitudes and the results are plotted in Fig. 6. The results indicate that the system has different dynamic performances with low input amplitudes (below 1 V) and high amplitudes. Realizing that the dead zone of the system is larger than 1 V under the major leakage condition, the system is operated with amplitude higher than 1 V in the later tests.

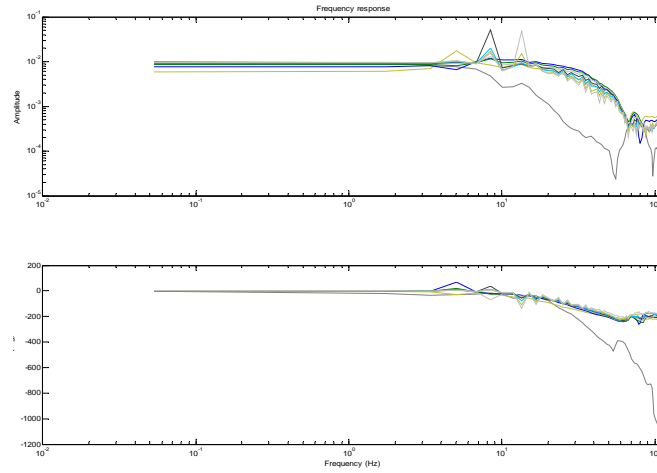


**Figure 6. Frequency response curves (amplitude and phase)**

The EHA system was found in [12] to be a third order system with an actuator velocity as an output. In this paper, the latest single value decomposition experiment results demonstrate that the system is a second order system with minor higher order dynamics, as shown in Fig. 7. Based on the prior knowledge obtained, a test input signal for data collection is designed as a 5 Hz pseudo random binary signal (PRBS) with zero mean and amplitude 4 V. The experimental output is filtered by a zero phase filter with 12<sup>th</sup>-order 30 Hz Butterworth low pass filter. Black box models are estimated with an output error model structure based on collected data for each working condition, as defined in Table 1. The system identification models are listed in the Appendix, and the performances of these models are validated in the model validation section.

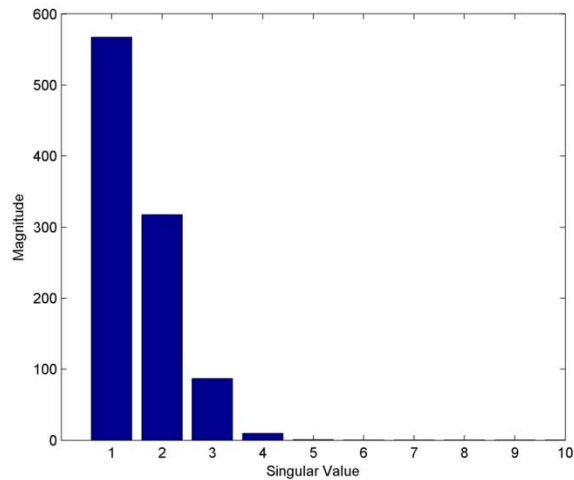


**Figure 7. Single value decomposition experiment results**

## 5 EHA Mathematical Modelling

In the previous section, linear models were obtained by implementing system identification techniques. However, these models are not able to capture the nonlinear system dynamics accurately. For comparison purposes, traditional mathematical modelling processes are implemented in this section. A mathematical model was developed and demonstrated for the EHA system in [4]. The mathematical model was then simplified further in [13]. The EHA pump flow is modeled as follows [13]:

$$Q_a = D_p \omega_p - \xi(P_a - P_b) - \frac{V_a}{\beta} \frac{dP_a}{dt} - C_{ep}(P_a - P_r) \quad (5.1)$$

$$Q_b = D_p \omega_p - \xi(P_a - P_b) + \frac{V_b}{\beta} \frac{dP_b}{dt} + C_{ep}(P_a - P_r) \quad (5.2)$$

In the equations above,  $Q_a, Q_b, P_a, P_b, V_a, V_b$  are: the pump flow rate, pressure and section volume associated with the inlet and outlet, respectively.  $\omega_p$  is the motor angular velocity.  $\xi$  is the pump cross-port leakage coefficient and  $C_{ep}$  is the pump external leakage coefficient.  $\beta$  stands for the effective bulk modulus of the working fluid while  $P_r$  is the accumulator pressure.  $V_a, V_b$  are assumed to be identical because the symmetrical design of the gear pumped in this study. The actuator flow is modeled by [13]:

$$Q_1 = A\dot{x} + \frac{A(x_0 + x)}{\beta} \frac{dP_1}{dt} + L_{in}(P_1 - P_2) + L_{out}(P_1) \quad (5.3)$$

$$Q_2 = A\dot{x} - \frac{A(x_0 - x)}{\beta} \frac{dP_2}{dt} + L_{in}(P_1 - P_2) - L_{out}(P_2) \quad (5.4)$$

where  $Q_1, Q_2, P_1, P_2$  are the actuator flow rate and pressure associated with the inlet and outlet, respectively.  $A$  is the effective piston area and  $x$  stands for the actuator displacement.  $L_{in}$  and  $L_{out}$  are the internal and external leakage coefficient. Since a steel pipeline is implemented in the prototype, the pressure loss and leakage due to the pipeline is assumed to be negligible. Therefore:

$$Q_a + Q_b = Q_1 + Q_2; P_1 = P_a, P_2 = P_b$$

Since the actuator is symmetrical,  $\frac{dP_1}{dt} = -\frac{dP_2}{dt}$ .  $V_0$  is the total mean volume given by  $V_0 = V_a + Ax_0$ . By substituting and simplifying, the flow rate model of the EHA is obtained as follows:

$$D_p \omega_p = A\dot{x} + \frac{V_0}{\beta} \left( \frac{dP_1}{dt} - \frac{dP_2}{dt} \right) + \left( L_{in} + \frac{L_{out}}{2} + \xi + \frac{C_{ep}}{2} \right) * (P_1 - P_2) \quad (5.5)$$

Using a lump sum leakage coefficient  $L_t = L_{in} + \frac{L_{out}}{2} + \xi + \frac{C_{ep}}{2}$ , the model can be further simplified as follows:

$$D_p \omega_p = A\dot{x} + \frac{V_0}{\beta} \left( \frac{dP_1}{dt} - \frac{dP_2}{dt} \right) + L_t(P_1 - P_2) \quad (5.6)$$

According to the model, the ideal pump flow  $D_p \omega_p$  contributes to the actuator motion  $A\dot{x}$ , fluid volume change  $\frac{V_0}{2\beta} \left( \frac{dP_1}{dt} - \frac{dP_2}{dt} \right)$ , and leakage  $L_t(P_1 - P_2)$ . At steady state one has  $\frac{dP_1}{dt} = \frac{dP_2}{dt} = 0$ , and the model can be transformed as follows:

$$L_t = \frac{D_p \omega_p - A\dot{x}}{P_1 - P_2} \quad (5.7)$$

According to the design of the EHA in [12], the values of the EHA parameters are listed in the following table.

Table 2. EHA parameters and their values

EHA Parameter	Description	Value
$D_p$	Gear pump volumetric displacement	$5.57 \times 10^{-7} \text{ m}^3/\text{s}$
$A$	Piston surface area	$1.52 \times 10^{-3} \text{ m}^2$
$V_0$	Nominal volume of each EHA chamber	$1.08 \times 10^{-3} \text{ m}^3$

In order to determine the leakage coefficient  $L_t$ , the EHA system is run with a constant velocity under different levels of differential pressure. The differential pressure is modified by changing the Axis B throttle valve input. Both the differential pressure and the actuator velocity are measured at steady state. The system leakage flow rate can be calculated by using (5.7). The experimental results regarding previously defined leakage conditions are plotted in Fig. 8.

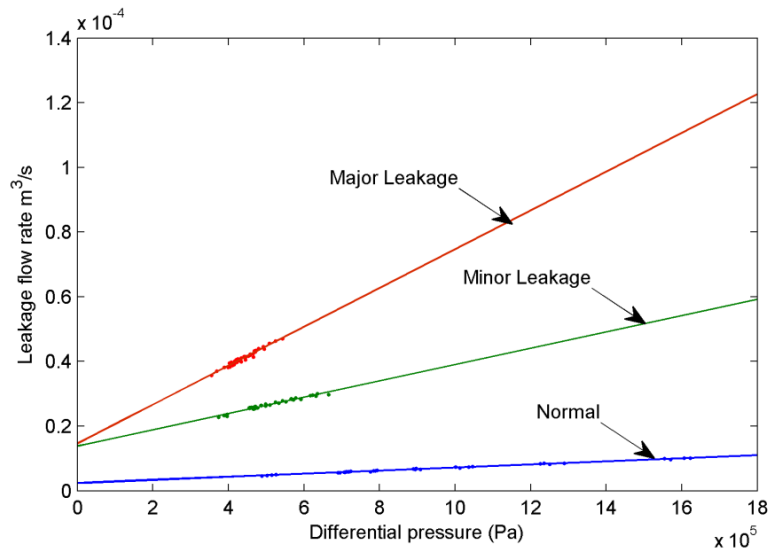


Figure 8. Various leakage flow rates based on condition

The leakage flow rate has a linear relationship with differential pressure which agrees with the mathematical model. However, a significant bias caused by the static friction of the system is also shown (with zero differential pressure). In order to calibrate the bias, the system model is modified as follows:

$$D_p \omega_p = A\dot{x} + \frac{V_0}{\beta} \left( \frac{dP_1}{dt} - \frac{dP_2}{dt} \right) + L_t(P_1 - P_2) + \text{sign}(\omega_p)Q_b \quad (5.8)$$

With  $L_t$  and  $Q_b$  calculated as per the following table.

Table 3. Leakage coefficients and flow rates

Condition	Leakage Coefficient	Flow Rate
Normal	$4.784 \times 10^{-12} \text{ Pa m}^3/\text{s}$	$2.413 \times 10^{-6} \text{ m}^3/\text{s}$
Minor Leakage	$2.523 \times 10^{-11} \text{ Pa m}^3/\text{s}$	$1.382 \times 10^{-5} \text{ m}^3/\text{s}$
Major Leakage	$6.006 \times 10^{-11} \text{ Pa m}^3/\text{s}$	$1.465 \times 10^{-5} \text{ m}^3/\text{s}$

In this paper, the EHA is not connected to any external load. The displacement of the actuator is related with the output force by the following equation:

$$F = (P_1 - P_2)A = M\ddot{x} + F_f \quad (5.9)$$

where  $M$  is the actuating mass which equals to  $7.376 \text{ kg}$  according to [12] and  $F_f$  is the actuator friction which can be described by a second order quadratic function related to the actuating velocity, as defined in [13]:

$$F_f = a_2\dot{x} + (a_1\dot{x}^2 + a_3)\text{sign}(\dot{x}) \quad (5.10)$$

At steady state, the acceleration of the actuator becomes zero and the force model can be modified as follows:

$$(P_1 - P_2)A = a_2\dot{x} + (a_1\dot{x}^2 + a_3)\text{sign}(\dot{x}) \quad (5.11)$$

To determine the friction coefficients  $a_1, a_2, a_3$ , experiments were performed with various randomly step inputs from  $0.5 \text{ V}$  to  $3.5 \text{ V}$ . Steady state velocity and differential pressures were measured and plotted regarding three previously defined friction conditions, as shown in Fig. 9. By best fitting the parabola curves into the data points, three friction models are extracted and are listed in the following table.

Table 4. Leakage coefficients and flow rates

Condition	$a_1$	$a_2$	$a_3$
Normal	$6.589 \times 10^4$	$2.144 \times 10^3$	436
Minor Friction	$1.162 \times 10^6$	$-7.440 \times 10^3$	500
Major Friction	$4.462 \times 10^6$	$1.863 \times 10^4$	551

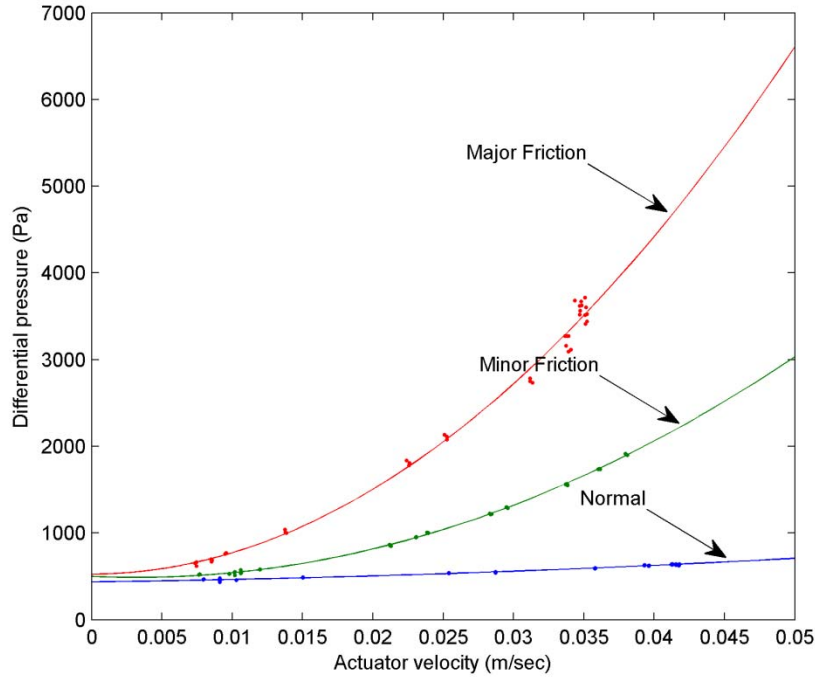


**Figure 9. Various friction rates based on condition**

Rearrange the force equation as follows:

$$P_1 - P_2 = \frac{M}{A} \ddot{x} + \frac{a_2}{A} \dot{x} + \frac{a_1 \dot{x}^2 + a_3}{A} \text{sign}(\dot{x}) \quad (5.12)$$

By assuming  $\text{sign}(\dot{x})$  as a constant then (5.12) becomes:

$$\frac{dP_1}{dt} - \frac{dP_2}{dt} = \frac{M}{A} \ddot{x} + \frac{a_2}{A} \dot{x} + \frac{2a_1 \dot{x} \ddot{x}}{A} \text{sign}(\dot{x}) \quad (5.13)$$

Substitution and rearranging yields the following:

$$D_p \omega_p - Q_b = \frac{MV_0}{A\beta} \ddot{x} + \frac{a_2 V_0 + M\beta L_t}{A\beta} \dot{x} + \frac{A^2 + a_2 L_t}{A} \dot{x} + \frac{2a_1 V_0 \dot{x} \ddot{x} + \beta L_t (a_1 \dot{x}^2 + a_3)}{A\beta} \text{sign}(\dot{x}) \quad (5.14)$$

## 6 Model Validation

The validation test input consists of nine sequential steps. The absolute amplitude of each step is a random number between 2.5 V to 4 V. Since the stroke of the actuator is limited, the actuating direction is switched after each step. The corresponding motor angular velocity is plotted as follows. The RMSE for each model is calculated based on the velocity measurement.

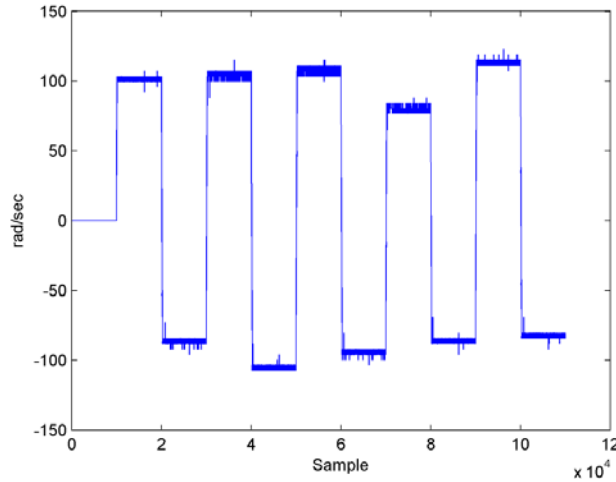


**Figure 10. System input used for model validation**

The following table lists the RMSE values for the models obtained mathematically and through system identification, as applied to the above signal under various conditions.

Table 5. Model validation

<b>Model / Condition</b>	<b>RMSE (System ID)</b>	<b>RMSE (Mathematical)</b>
Normal	0.0023	0.0015
Minor Friction	0.0023	0.0018
Major Friction	0.0035	0.0014
Minor Leakage	0.0027	0.0011
Major Leakage	0.0044	0.0013
Min. L & Min. F	0.0018	0.0013
Min. L & Maj. F	0.0012	0.0011
Maj. L & Min. F	0.0032	0.0007
Maj. L & Maj. F	0.0029	0.0011

As demonstrated in the above table, the models obtained mathematically yielded the best fit to the measurements. This is expected since the models from the system ID are linear, whereas the mathematical models better capture the nonlinearities present in the system.

## 7 Bulk Modulus Estimation

Hydraulic fluid is incompressible when it is considered as ideal (i.e., no air bubbles present). With the presence of air, the fluid become compressible and causes slower response of the system and losses of energy. The parameter effective bulk modulus  $\beta$  is a measure of the fluid resistance to compression. It is difficult to determine the effective bulk modulus experimentally since the volume of air trapped in the system is unpredictable. In such cases, the popular extend Kalman filter may be used with the mathematical model to estimate the effective bulk modulus [13]. In an effort to implement the EKF, the system model is transformed into the following state space equations. Note however that the EKF equations may be found in [13,15], and were omitted due to space constraints.

$$x_{1,k+1} = x_{1,k} + Tx_{2,k} \quad (7.1)$$

$$x_{2,k+1} = x_{2,k} + Tx_{3,k} \quad (7.2)$$

$$x_{3,k+1} = \left[ 1 - T \frac{a_2 V_0 + M L_t x_{4,k}}{M V_0} \right] x_{3,k} - T \frac{A^2 + a_2 L_t}{M V_0} x_{4,k} x_{2,k} - T \left[ \frac{2a_1 x_{2,k} x_{3,k}}{M V_0} + \frac{(a_1 x_{2,k}^2 + a_3) L_t}{M V_0} x_{4,k} \right] \text{sign}(x_{2,k}) \quad (7.3)$$

$$+ T \left[ \frac{A(D_p \omega_p - \text{sign}(\omega_p) Q_b)}{M V_0} x_{4,k} \right] \quad (7.4)$$

$$x_{4,k+1} = x_{4,k}$$

Note that the linearized system matrix is defined as follows:

$$\varphi(k) = \frac{\partial f(x(k))}{x(k)} = \begin{bmatrix} \varphi_{11}(k) & \varphi_{12}(k) & \varphi_{13}(k) & \varphi_{14}(k) \\ \varphi_{21}(k) & \varphi_{22}(k) & \varphi_{23}(k) & \varphi_{24}(k) \\ \varphi_{31}(k) & \varphi_{32}(k) & \varphi_{33}(k) & \varphi_{34}(k) \\ \varphi_{41}(k) & \varphi_{42}(k) & \varphi_{43}(k) & \varphi_{44}(k) \end{bmatrix} \quad (7.5)$$

where the parameters of (7.5) are defined by:

$$\begin{aligned} \varphi_{11}(k) &= 1; \varphi_{21}(k) = T; \varphi_{31}(k) = 0; \varphi_{41}(k) = 0; \varphi_{21}(k) = 0; \varphi_{22}(k) = 1; \\ \varphi_{23}(k) &= T; \varphi_{24}(k) = 0; \varphi_{31}(k) = 0; \\ \varphi_{32}(k) &= -T \text{sign}(x_{2,k}) \left( \frac{2a_1 x_{3,k}}{M} + \frac{2a_1 L_t x_{2,k} x_{4,k}}{M V_0} \right) - T \frac{A^2 + a_2 L_t}{M V_0} x_{4,k}; \\ \varphi_{33}(k) &= 1 - T \frac{2a_1}{M} x_{2,k} \text{sign}(x_{2,k}) - T \frac{a_2 V_0 + L_t M x_{4,k}}{M V_0}; \\ \varphi_{34}(k) &= T \frac{A u_k}{M V_0} - T \frac{x_{2,k} (A^2 + a_2 L_t)}{M V_0} - T \frac{L_t}{V_0} x_{3,k} - T \frac{L_t (a_1 x_{2,k}^2 + a_3)}{M V_0} \text{sign}(x_{2,k}); \\ \varphi_{41}(k) &= 0; \varphi_{42}(k) = 0; \varphi_{43}(k) = 0; \varphi_{44}(k) = 1; \\ u_k &= D_p \omega_p(k) - \text{sign}(\omega_p) Q_b; \end{aligned}$$

Furthermore,  $T$  is the sampling time used in this paper, and was set to 0.1 ms. Note that the system and measurement noise covariance matrices were defined respectively as follows:

$$Q = \text{diag}(1 \times 10^{-12} \ 1 \times 10^{-8} \ 1 \times 10^{-6} \ 1 \times 10^{-12}) \quad (7.6)$$

$$R = \text{diag}(1 \times 10^{-12} \ 1 \times 10^{-4}) \quad (7.7)$$

The input with the higher frequency can excite the system better for more accurate bulk modulus estimation [13]. However, based on the experiments performed in system identification, the bandwidth of the EHA is around 25 Hz. The EHA system dynamics change significantly at a higher frequency region due to the dead-band and nonlinear friction. The testing input is chosen as a sinusoidal wave with 4 V amplitude and 10 Hz frequency. The corresponding motor angular velocity range is  $\pm 1200$  RPM. Note that the two measurements include piston displacement and velocity. The bulk modulus estimation process is executed with initial bulk modulus values from 0 Pa to  $5 \times 10^8$  Pa, and the result is plotted in Fig. 11. The bulk modulus values converge to the same value  $2.07 \times 10^8$  Pa which agrees with the bulk modulus value  $2.1 \times 10^8$  Pa obtained in [13].

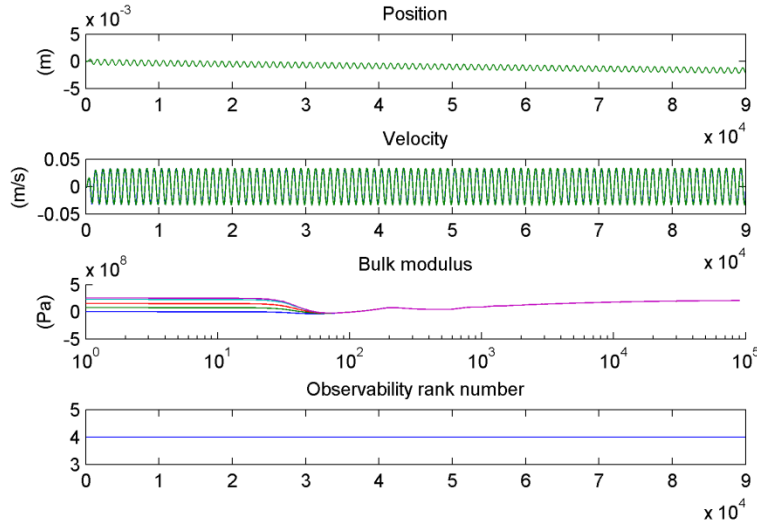


**Figure 11. Effective bulk modulus estimation of the EHA using the EKF**

## 6 Conclusion

In this paper, an EHA built for experimentation is studied. System models based on a number of conditions were generated mathematically as well as through system identification. It was found that the mathematical models were better able to capture the nonlinearity of the EHA system. These models were validated based on experimental results obtained from the EHA setup. The effective bulk modulus of the system was estimated using the EKF, and the results confirmed the values obtained in earlier studies.

## 7 Appendix

The following is a list of the EHA models obtained through system identification.

Table 6. Models Obtained by System Identification

Operating Condition	System ID Model
Normal	$\frac{0.0001977z^2 - 0.000361z + 0.0001635}{z^2 - 1.893z + 0.894}$
Minor Friction	$\frac{0.0003197z^2 - 0.0006023z + 0.0002867}{z^2 - 1.747z + 0.7646}$
Major Friction	$\frac{0.0003089z^2 - 0.0005827z + 0.0002763}{z^2 - 1.675z + 0.6906}$
Minor Leakage	$\frac{4.137e - 6z^2 + 5.574e - 5z - 5.912e - 5}{z^2 - 1.755z + 0.7577}$
Major Leakage	$\frac{0.0002287z^2 - 0.0004551z + 0.0002331}{z^2 - 1.883z + 0.9092}$
Min. L & Min. F	$\frac{0.000208z^2 - 0.0004107z + 0.0002086}{z^2 - 1.905z + 0.9356}$
Min. L & Maj. F	$\frac{0.0001352z^2 - 0.0002643z + 0.0001323}{z^2 - 1.943z + 0.9619}$
Maj. L & Min. F	$\frac{(0.0001897z^2 - 0.0003723z + 0.0001877)}{z^2 - 1.933z + 0.9738}$
Maj. L & Maj. F	$\frac{(0.0001016z^2 - 0.0001982z + 9.692e - 5)}{z^2 - 1.959z + 0.9621}$

## 8 References

- [1] J. F. Blackburn, G. Reethof, and J. L. Shearer, *Fluid Power Control*. Boston, U.S.A.: MIT Press, 1960.
- [2] H. E. Merritt, *Hydraulic Control Systems*. New York, U.S.A.: John Wiley & Sons, Inc., 1967.
- [3] T. J. Viersma, *Analysis, Synthesis, and Design of Hydraulic Servo-Systems and Pipelines*.: Elsevier Scientific Publishing Company, 1980.
- [4] S. R. Habibi and A. Goldenberg, "Design of a New High-Performance Electrohydrostatic Actuator," *IEEE/ASME Transactions on Mechatronics*, vol. 5, no. 2, pp. 158-164, June 2000.
- [5] S. R. Habibi, R. Richards, and A. Goldenberg, "Hydraulic Actuator Analysis for Industrial Robot Multivariable Control," in *American Control Conference*, 1994, pp. 1003-1007.
- [6] S. R. Habibi and R. Richards, "Computed-Torque and Variable-Structure Multivariable Control of a Hydraulic Industrial Robot," in *Inst. Mechanical Engineering*, 1991, pp. 123-140.
- [7] S. R. Habibi, "High Precision Hydrostatic Actuation Systems for Micro and Nano Manipulation of Heavy Loads," *ASME Journal of Dynamic Systems, Measurement and Control*, vol. 128, December 2006.
- [8] L. Ljung, *System Identification: Wiley Encyclopedia of Electrical and Electronics Engineering*. New York, U.S.A.: Wiley & Sons, Inc., 1999.
- [9] S. R. Habibi, "System Identification: Part 1," McMaster University, Hamilton, Ontario, Graduate Mechatronics Course Lecture 2010.
- [10] S. R. Habibi, "The Smooth Variable Structure Filter," *Proceedings of the IEEE*, vol. 95, no. 5, pp. 1026-1059, 2007.

- [11] M. El Sayed, "Multiple Sliding Mode Control for Electro-Hydraulic Actuation (EHA) Systems," *Article Under Preparation*, 2011.
- [12] K. McCullough, "Design and Characterization of a Dual Electro-Hydrostatic Actuator," Department of Mechanical Engineering, McMaster University, Hamilton, Ontario, M.A.Sc. Thesis 2011.
- [13] Y. A. Chinniah, "Fault Detection in the Electrohydraulic Actuator Using the Extended Kalman Filter," Department of Mechanical Engineering, University of Saskatchewan, Saskatoon, Saskatchewan, Ph.D. Thesis 2004.
- [14] S. R. Habibi and R. Burton, "Parameter Identification for a High Performance Hydrostatic Actuation System using the Variable Structure Filter Concept," *ASME Journal of Dynamic Systems, Measurement, and Control*, 2007.
- [15] S. A. Gadsden, "Smooth Variable Structure Filtering: Theory and Applications," Department of Mechanical Engineering, McMaster University, Hamilton, Ontario, Ph.D. Thesis 2011.